Breakout from the hot CNO cycle: The ^{18}F(p,γ) vs ^{18}F(p,α) branching ratio

S. Utku,[1,*] J. G. Ross,[2,†] N. P. T. Bateman,[1,‡] D. W. Bardayan,[1] A. A. Chen,[1] J. Görres,[2] A. J. Howard,[3] C. Iliadis,[2,§]
P. D. Parker,[1] M. S. Smith,[4] R. B. Vogelaar,[5] M. Wiescher,[2] and K. Yildiz[1]

[1]*Wright Nuclear Structure Laboratory, Yale University, New Haven, Connecticut 06520-8124*
[2]*Department of Physics, University of Notre Dame, Notre Dame, Indiana 46556*
[3]*Physics Department, Trinity College, Hartford, Connecticut 06106*
[4]*Physics Division, Oak Ridge National Laboratory, Oak Ridge, Tennessee 37831*
[5]*Department of Physics, Princeton University, Princeton, New Jersey 08544*

We have studied the properties of low-lying ^{18}F$+p$ resonances as excited states in ^{19}Ne. Three new levels have been found in the range $0 \leq E_{c.m.} \leq 1$ MeV just above the ^{18}F$+p$ threshold, and partial decay widths and isospin-mirror connections are suggested to known states in ^{19}F for each of the nine states in this energy range. The properties of these resonances have been used to calculate the reaction rate $N_A\langle\sigma v\rangle$ for the ^{18}F$(p,\gamma)^{19}$Ne and ^{18}F$(p,\alpha)^{15}$O reactions in the temperature range $10^8 < T < 10^9$. A comparison of these rates indicates that in this temperature range, the ^{14}O$(\alpha,p)^{17}$F$(p,\gamma)^{18}$Ne$(e^+\nu)^{18}$F$(p,\gamma)^{19}$Ne reaction sequence is not as fast as the ^{15}O$(\alpha,\gamma)^{19}$Ne reaction. [S0556-2813(98)06305-5]

PACS number(s): 26.30.+k, 25.40.Ny, 27.20.+n

I. INTRODUCTION

Classical nova explosions are powered by the hot CNO cycle [1] which is initiated on the surfaces of accreting white dwarfs when temperatures and densities become sufficiently high so that the ^{13}N$(p,\gamma)^{14}$O reaction becomes fast enough to bypass the beta decay of ^{13}N. At still higher temperatures and densities, the ^{14}O$(\alpha,p)^{17}$F and ^{15}O$(\alpha,\gamma)^{19}$Ne reactions will become fast enough so that the reaction flow will bypass the beta decays of ^{14}O and ^{15}O and result in either a faster hot CNO cycle or a breakout from that cycle to the rp process [2,3], increasing the rate of explosive energy generation and leading to the nucleosynthesis of much higher-Z material.

In the possible breakout from the hot CNO cycle to the rp process via the ^{14}O$(\alpha,p)^{17}$F reaction, ^{18}F can be reached via the sequence ^{14}O$(\alpha,p)^{17}$F$(p,\gamma)^{18}$Ne$(e^+\nu)^{18}$F. By taking advantage of the high ^{16}O abundance on the surface of a white dwarf, ^{18}F can also be produced via the reaction sequence ^{16}O$(p,\gamma)^{17}$F$(p,\gamma)^{18}$Ne$(e^+,\nu)^{18}$F. It is then necessary to measure the branching ratio between the ^{18}F$(p,\gamma)^{19}$Ne and ^{18}F$(p,\alpha)^{15}$O reactions in order to determine if these sequences continue on towards the rp process or return to the hot CNO cycle. The resonant contributions to the rates of these two competing reactions are determined by the properties of the levels in the ^{19}Ne compound nucleus just above the ^{18}F$+p$ threshold. From a comparison between the known levels in this region in ^{19}Ne and in its well-studied isospin mirror ^{19}F [4], it was clear that 9 out of the 15 ^{19}Ne levels expected in this region ($6.4 \leq E_x \leq 7.4$ MeV) had not been located at the start of this study. Therefore, we have undertaken a series of measurements to search for these missing resonances and to determine the spectroscopic properties of the ^{19}Ne states in this region either by direct measurements or by establishing their isospin-mirror connections to known levels in ^{19}F.

II. EXPERIMENTAL MEASUREMENTS

A. ^{19}F$(^3$He,$t)^{19}$Ne reaction

In order to search for missing ^{19}Ne states in the region just above the ^{18}F$+p$ threshold and to determine precise resonance energies for the states in this region, measurements of the ^{19}F$(^3$He,$t)^{19}$Ne reaction were made using the Notre Dame Browne-Buechner spectrograph [5] and the Princeton QDDD spectrometer [6]. In these measurements, 29.8-MeV ^{3}He beams were used to bombard CaF$_2$ targets (50 μg/cm^2 evaporated onto 10 μg/cm^2 carbon foils), and the resulting tritons (selected on the basis of $\Delta E \times E$ particle identification at the focal plane) were measured at 0°, 5°, 10°, and 15°, with a full width at half maximum (FWHM) resolution of 24 keV; tritons from the ^{27}Al$(^3$He,$t)^{27}$Si reaction were measured at the same spectrometer settings at 10° in order to calibrate the ^{19}Ne spectra with a precision of ±5 keV. As an example of these data, the 10° ^{19}F$(^3$He,$t)^{19}$Ne spectrum is plotted in Fig. 1, and the resulting level energies extracted from these data and from the higher-statistics data from the subsequent coincidence measurements at 0° are listed in Table I. Attempts to analyze the peak at 7.070 MeV as an unresolved doublet did not produce any significant improvement over a single-level fit to this peak; nor was there any indication of shifts in the position or shape of this peak as a function of angle from 0° to 15°; nor was there any significant difference in the proton/alpha-particle branching ratio (Γ_p/Γ_α), as measured in Sec. II B, for slices taken at

---

*Present address: Columbia University Law School, Columbia University, New York, NY 10027.

†Present address: Department of Physics and Astronomy, University of Central Arkansas, Conway, AR 70235.

‡Present address: TRIUMF, Vancouver, B.C. V6T 2A3, Canada.

§Present address: Department of Physics and Astronomy, University of North Carolina, Chapel Hill, NC 27599.
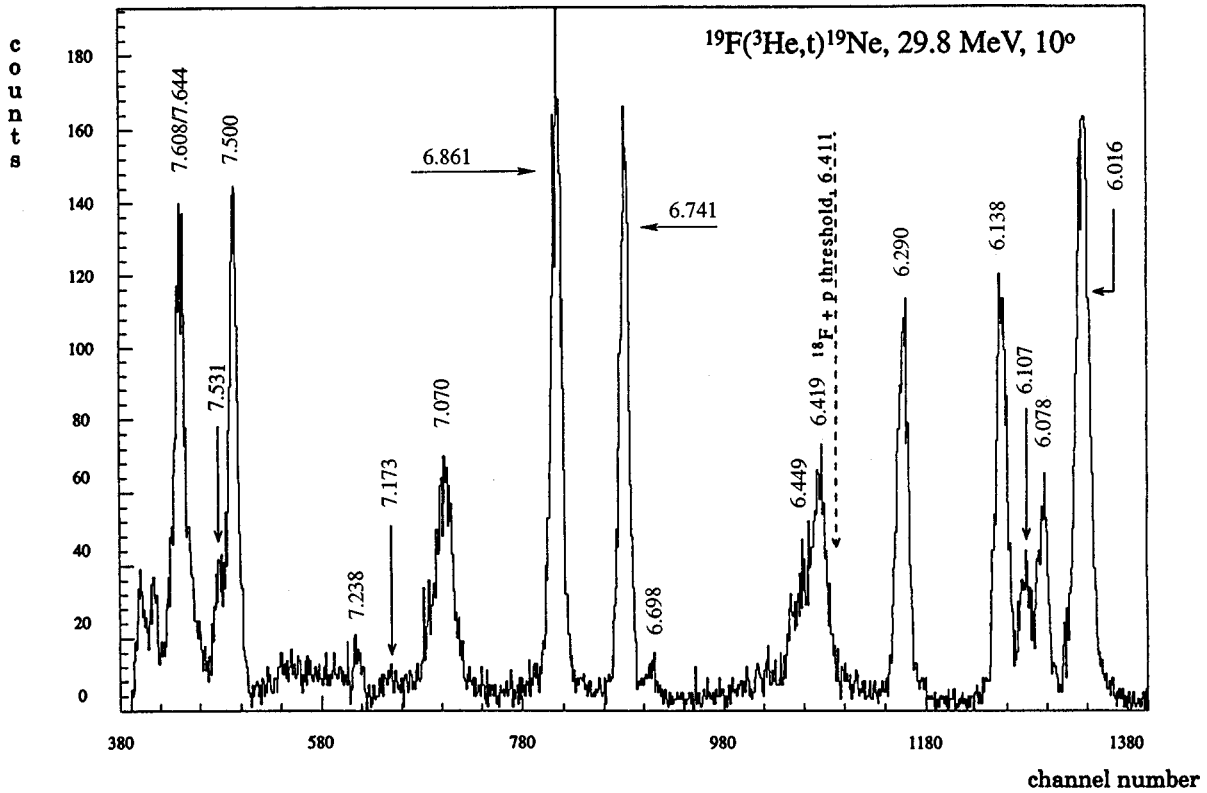
FIG. 1. ^{19}F(^{3}He,t)^{19}Ne spectrum measured at $\theta_{lab}=10°$ for an incident ^{3}He energy of 29.8 MeV at the Princeton cyclotron facility. The peaks are labeled with the excitation energies of the corresponding states in ^{19}Ne. The location of the ^{18}F+p threshold is indicated.

various positions in this peak. For example, for the high- and low-energy halves of the peak, the α/p coincidence ratio was measured as 1.85 ± 0.35 and 2.45 ± 0.50, respectively. In our analysis of these data, the peak at $E_x=7.070$ MeV has therefore been treated as due to a single state with a measured width $\Gamma_{tot}=\sqrt{(46)^2-(24)^2}=39(\pm10)$ keV. The *relative* heights of the peaks in Fig. 1 did not change significantly as a function of angle in the measured spectra from 0° to 15° and therefore did not provide a sensitive way to investigate

the J^π of this state; a more sensitive way is a comparison of a measurement of the proton partial width of the state with the appropriate single-particle Wigner limit (see Sec. II D below).

Finally, it should noted that although three new levels were found in the region $6.4\leq E_x\leq7.4$ MeV, six levels are still missing in this region and need to be identified in order to determine the resonant reaction rates for the ^{18}F(p,γ)^{15}O and ^{18}F(p,γ)^{19}Ne reactions. As described below in Sec.

TABLE I. ^{19}Ne level properties.

	Present experiment			
E_x (MeV) [a]	E_x (MeV)	Γ_α/Γ	Γ_p/Γ	Γ_{tot} (keV)
	6.419(6)			
6.437(9)	6.437(9)			216(19)
	6.450(6)			
	6.698(6)			
6.742(7)	6.741(6)	1.04 ± 0.08		
6.861(7)	6.861(6)	0.96 ± 0.08	<0.025	
7.067(9)	7.070(7)	0.64 ± 0.06	0.37 ± 0.04	39(10)
7.21(20)	7.173(5)			
7.253(10)	7.238(6)			
[7.326(15)]				
	7.500(9)	0.16 ± 0.02	0.84 ± 0.04	16(16)
[7.531(15)]	7.531(11)	0.67 ± 0.08	0.33 ± 0.06	31(16)
7.616(16)	7.608(11)	0.97 ± 0.04	0.04 ± 0.02	45(16)
	7.644(12)	0.37 ± 0.06	0.64 ± 0.04	43(16)
	7.819(11)	0.19 ± 0.09	0.81 ± 0.11	22(16)

[a]Reference [4].

II C, we have also carried out studies of this region of ^{19}Ne using the ^{16}O(^{6}Li,t) and ^{20}Ne(d,t) reactions, but no additional new states were found. Additional studies using reactions, such as ^{12}C(^{13}C,^{6}He), ^{12}C(^{10}B,t), and ^{19}F(^{6}Li,^{6}He), are planned.

B. ^{19}F(^{3}He,$t\alpha$)^{15}O and ^{19}F(^{3}He,tp)^{18}F coincidence measurements

We have carried out coincidence measurements of the ^{19}F(^{3}He,$t\alpha$)^{15}O and ^{19}F(^{3}He,tp)^{18}F reactions, in order to determine the proton and alpha-particle partial decay widths Γ_p/Γ and Γ_α/Γ of individual ^{18}F+p resonances. A 29.8-MeV ^{3}He beam from the Princeton cyclotron was used to bombard a 50-μg/cm^2 CaF$_2$ target, and the resulting tritons were detected at 0° with the Princeton QDDD spectrometer; in this geometry, the residual ^{19}Ne nuclei have recoil energies of only $\approx$200 keV. The coincident protons and alpha particles were measured with Si(SB) detectors (nominally 450 mm^2, covering 52 msr) centered at laboratory angles of 90°, 110°, and 145°. The product of solid angle and efficiency was measured for each of the Si(SB) detectors using coincidences from the ^{19}F(^{3}He,$d\alpha$)^{16}O reaction through the 6.725-MeV, $J^\pi=0^+$ excited state in ^{20}Ne; except for a 2 $\times10^{-6}$ gamma-decay branch, this state decays 100% by alpha-particle emission to the ground state of ^{16}O, and the emitted alpha particles have an isotropic angular distribution in the recoil center-of-mass frame.

Software gates were set on the "true-coincidence" peak (typically, $\approx$16 ns, FWHM) in the triton$\otimes$(p/α) time-to-amplitude converter (TAC) spectrum, for each of the triton groups of interest and for each of the Si(SB) detectors (e.g., Fig. 2). These gates were used to generate the coincident proton/alpha-particle spectra for each triton group at each angle (e.g., Fig. 3). Random-coincidence spectra were generated for each Si(SB) detector for each triton group by gating on ten cyclotron beam bursts, away from the "true-coincidence" peak, and one-tenth of the resulting counts in the proton and alpha-particle peak positions were subtracted from the corresponding coincidence spectrum. The resulting net proton and alpha-particle yields were corrected for the efficiency and solid angle of each Si(SB) detector and then converted into the center-of-mass frame of the ^{19}Ne recoil and fit with a linear combination of $l=0$, 2, and 4 Legendre polynomials. Integrating these Legendre polynomials over 4π determines the total yield of decay protons and alpha particles for each triton group and thereby its Γ_p/Γ and Γ_α/Γ decay branching ratios. These measured branching ratios are listed in Table I.

C. Comparison of the ^{16}O(^{6}Li,t)^{19}Ne and ^{16}O(^{6}Li,^{3}He)^{19}F reactions and the ^{20}Ne(d,t)^{19}Ne and ^{20}Ne(d,^{3}He)^{19}F reactions

For those cases in which we were not able to measure directly some particular properties of the ^{18}F+p resonances, it is often possible to determine those properties from a transformation of the corresponding properties for the specific isospin-mirror states in ^{19}F. In order to make isospin-mirror identifications between states in ^{19}Ne and ^{19}F, we have measured the two sets of mirror reaction pairs,
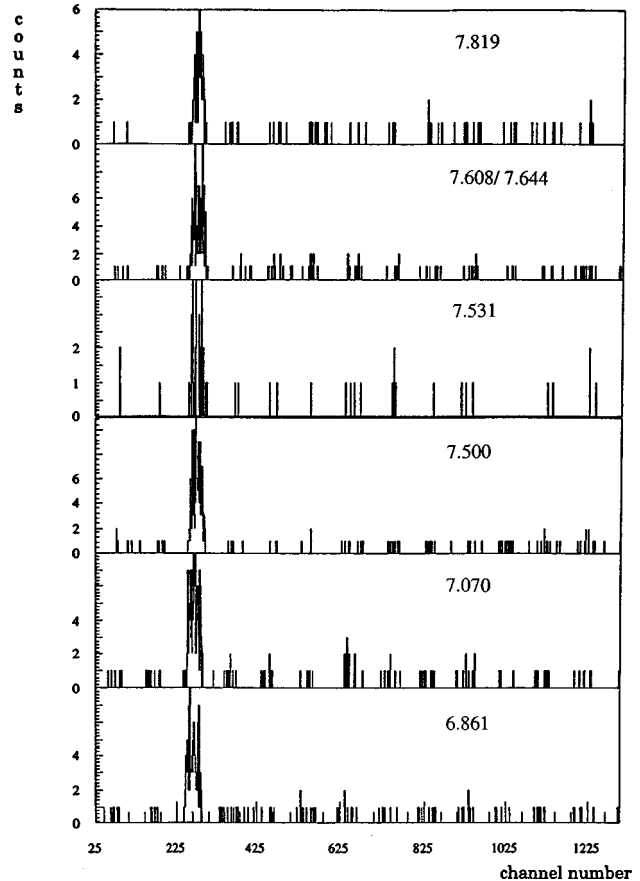

FIG. 2. TAC spectra for coincidence measurements between tritons at the focal plane of the Princeton QDDD (at 0°) and protons and alpha particles measured with a Si(SB) detector at an angle of 145°, in the target chamber. Each spectrum is labeled with the excitation energy of the corresponding ^{19}Ne state.

$$^{16}\text{O}(^{6}\text{Li},t)^{19}\text{Ne} \quad \text{vs} \quad ^{16}\text{O}(^{6}\text{Li},^{3}\text{He})^{19}\text{F}$$

and

$$^{20}\text{Ne}(d,t)^{19}\text{Ne} \quad \text{vs} \quad ^{20}\text{Ne}(d,^{3}\text{He})^{19}\text{F},$$

using 32-MeV ^{6}Li beams from the Notre Dame tandem accelerator and 28-MeV ^{6}Li beams and 30-MeV ^{2}H beams from the Yale tandem accelerator. The ^{16}O(^{6}Li,t) and ^{16}O(^{6}Li,^{3}He) reactions were measured using WO$_3$ targets (200 μg/cm^2 evaporated onto 500-μg/cm^2 gold foils at Notre Dame and 80 μg/cm^2 evaporated onto 300-μg/cm^2 gold foils at Yale); in order to check the kinetic shifts of the observed peaks, measurements were made at two angles (at 7.5° and 14° at Notre Dame and at 8° and 11° at Yale). The ^{20}Ne(d,t) and ^{20}Ne(d,^{3}He) reactions were measured at seven angles in the range $12.5° < \Theta_{lab} < 45°$ with a target of enriched (99.95%) ^{20}Ne in a gas cell, using Si(SB) detectors in a scattering chamber. A subsequent measurement was then made at $\Theta_{lab}=20°$ at higher resolution in a magnetic spectrometer, using an implanted target (7 μg/cm^2 of ^{20}Ne implanted in a 40-μg/cm^2 carbon foil).

The selectivity of these reaction pairs is evident in Figs. 4 and 5; for example, in Fig. 4 only roughly half of the resolvable states in this region of ^{19}F are populated in this spectrum. A comparison of previously estab-
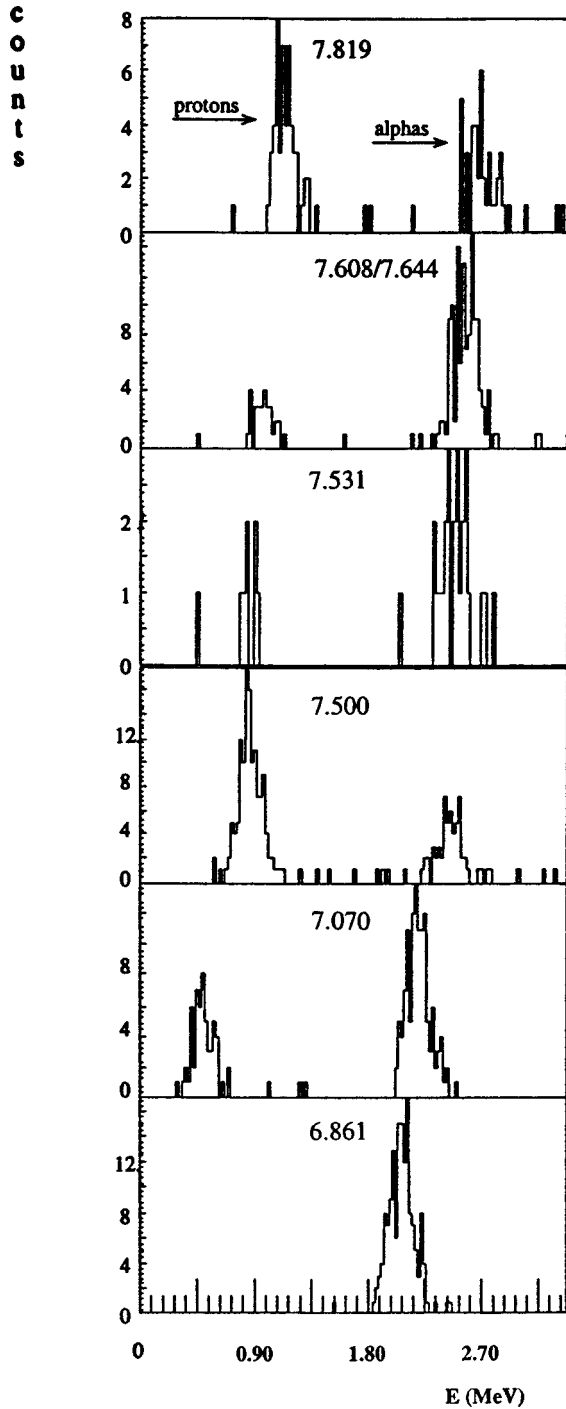
FIG. 3. The energy spectra for the coincident particles (protons and alpha particles) measured in a Si(SB) detector at an angle of 145°. The protons and alpha particles both stop in the detector and are clearly separated by their different energies. Each spectrum is labeled with the excitation energy of the corresponding ^{19}Ne state. (The shift in these particle energies with excitation energy is clearly visible.)

lished mirror states [such as ^{19}Ne(2.795)$\Leftrightarrow$^{19}F(2.780), ^{19}Ne(4.140 and 4.197)$\Leftrightarrow$^{19}F(3.999 and 4.033), and ^{19}Ne(5.424)$\Leftrightarrow$^{19}F(5.464)] supports the mirror nature of these reaction pairs. (See also Ref. [7].) On this basis, in the range $6.4 \leqslant E_x(^{19}\text{Ne}) \leqslant 7.4$ MeV, a comparison of the ^{16}O(^{6}Li,t)^{19}Ne and ^{16}O(^{6}Li,^{3}He)^{19}F spectra in Fig. 4 suggests isospin-mirror pair identifications for the
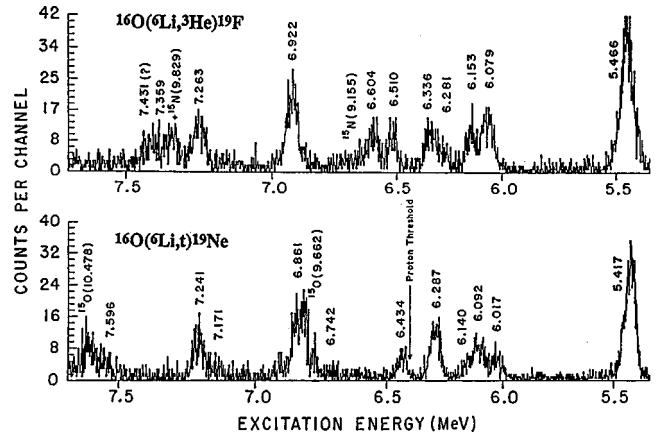
FIG. 4. Mirror spectra for the ^{16}O(^{6}Li,^{3}He)^{19}F and ^{16}O(^{6}Li,t)^{19}Ne reactions, measured at $\theta_{\text{lab}}=14°$ for an incident ^{6}Li energy of 32 MeV from the Notre Dame FN Tandem. The peaks are labeled with the excitation energies of the corresponding states in ^{19}F and ^{19}Ne.

^{19}Ne(6.861)$\Leftrightarrow$^{19}F(6.927)   and ^{19}Ne(7.238)$\Leftrightarrow$ ^{19}F(7.262) states. Similarly, a comparison of the ^{20}Ne(d,t)^{19}Ne and ^{20}Ne($d,^3$He)^{19}F spectra in Fig. 5 suggests an isospin-mirror pair identification for the ^{19}Ne(6.741)$\Leftrightarrow$^{19}F(6.787) states; the measured angular distributions for these two states are also identical.

The results of the ^{19}F(^{3}He,t) measurements, together with the results of these mirror reaction studies, are summarized in the $A=19$ level diagram in Fig. 6. In addition to the
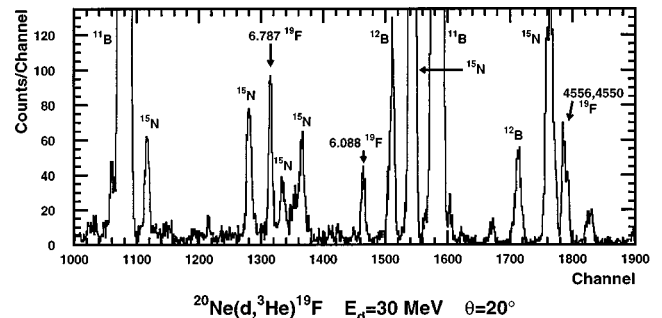
FIG. 5. Mirror spectra for the ^{20}Ne($d,^3$He)^{19}F and ^{20}Ne(d,t)^{19}Ne reactions, measured at $\theta_{\text{lab}}=20°$ for an incident deuteron energy of 30 MeV from the Yale ESTU Tandem. The peaks are labeled with the excitation energies of the corresponding states in ^{19}F and ^{19}Ne.
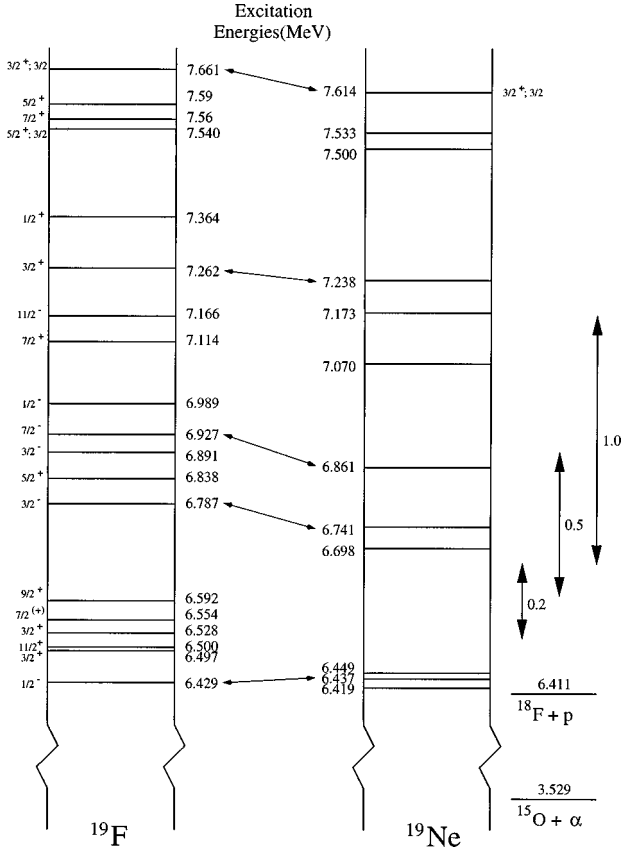
FIG. 6. Comparison of the level structure in ^{19}F and ^{19}Ne in the region just above the ^{18}F$+p$ threshold. Isospin-mirror state connections for the ^{19}Ne states at 6.741, 6.861, and 7.238 MeV are indicated based on relative populations and angular distributions measured for the ^{20}Ne$(d,^3$He$)^{19}$F and ^{20}Ne$(d,t)^{19}$Ne reactions and for the ^{16}O$(^6$Li,^{3}He$)^{19}$F and ^{16}O$(^6$Li,$t)^{19}$Ne reactions. The location (E_0) and width (ΔE_0) of the Gamow peak are indicated for temperatures of $T_9 = 0.2$, 0.5, and 1.0.

suggested mirror assignments discussed above, the ^{19}Ne(6.437)$\Leftrightarrow^{19}$F(6.429) states are also suggested as a possible mirror pair on the basis of their similar decay widths and excitation energies. It should be noted, however, that at least six ^{19}Ne levels are still missing in the region $6.4 \leq E_x \leq 7.4$ MeV and need to be identified in order to more accurately determine the resonant reaction rates for the ^{18}F$(p,\alpha)^{15}$O and ^{18}F$(p,\gamma)^{19}$Ne reactions.

D. Isospin mirror for ^{19}Ne*(7.070) in ^{19}F

A comparison of the measured proton partial width for the 7.070-MeV state $\Gamma_p = 14(\pm 4)$ keV with the single-particle Wigner limits for this state for various choices of J^π [8] favors a $J^\pi = 1/2^+$, $3/2^+$ ($l=0$) assignment for this state. In considering the identification of a ^{19}F mirror state for the ^{19}Ne(7.070) state, it has recently been pointed out [8,9] that a ^{15}N(α,α) elastic scattering study [10] of this region in ^{19}F had suggested that there might be an unresolved $3/2^+$, $7/2^+$ doublet at $E_x = 7.1$ MeV whose $3/2^+$ member would then be an attractive candidate for the ^{19}F mirror of the ^{19}Ne(7.070) state. However, more recent studies of this region in ^{19}F, including a reanalysis [11] of the scattering data of Smotrich et al. [10] and a ^{15}N(α,γ) study [12], have not found evidence for the putative $3/2^+$ state. This is clearly a critical

question in interpreting our results and the recent ^{18}F-beam results [8,9], and additional studies need to be focused on this issue.

III. REACTION RATES

In making (p,α) and (p,γ) reaction rate calculations for all the ^{18}F$+p$ resonances that have now been located in ^{19}Ne, we have made use of the measured total and partial widths (where available) together with information from the appropriate isospin-mirror states in ^{19}F. In cases where the mirror state has not been established or where the particular property has not been measured for either the ^{19}Ne state or the ^{19}F state, we have had to make ''educated guesses'' based on averages or the systematic properties of nuclear states in this region. These educated guesses can lead to rates for specific individual resonances which may be overestimated or underestimated by as much as a factor of 10.

The resulting parameters are summarized in Table II for the nine resonances in the range $0 \leq E_{c.m.} \leq 1.0$ MeV, (6.4 $\leq E_x \leq 7.4$ MeV). For these resonances, the Γ_γ values are taken either from the measured values for the mirror states in ^{19}F or, for cases in which there are no measured values for the mirror states, a value of $\Gamma_\gamma = 1$ eV was assumed, based on the average of the measured values for the ^{19}F states in this region. For the resonances for which we were not able to extract the proton width from our data, Γ_p was calculated by using the experimental single-particle spectroscopic factors Θ_p^2 obtained for the mirror states in ^{19}F [13]. However, for many of these levels, only upper limits for the spectroscopic factors have been determined. In those cases, we assumed a value of $\Theta_p^2 = 0.1$ for positive parity states and $\Theta_p^2 = 0.01$ for negative parity states [14]. For the resonances for which we were not able to extract the alpha width from our data, Γ_α was calculated from the alpha width of the mirror state in ^{19}F by assuming that the mirror states have the same reduced alpha widths, Θ_α^2, and then correcting for the different Coulomb barrier penetrations,

$$(\Gamma_\alpha)_{^{19}\text{Ne}} = \left[\frac{\rho}{F_l^2 + G_l^2} \right]_{^{15}\text{O}+\alpha} \left[\frac{F_l^2 + G_l^2}{\rho} \right]_{^{15}\text{N}+\alpha} (\Gamma_\alpha)_{^{19}\text{F}}. \quad (1)$$

The resulting ^{18}F(p,γ) and (p,α) resonance strengths $\omega\gamma_{(p,\gamma)}$ and $\omega\gamma_{(p,\alpha)}$ are listed in Table II, where,

$$(\omega\gamma)_{xy} = \frac{(2J_R+1)}{(2s_1+1)(2s_2+1)} \frac{\Gamma_x\Gamma_y}{\Gamma_{tot}}. \quad (2)$$

In Table II, it should be noted (1) that there are still six ^{19}F states in this region for which no corresponding ^{19}Ne states have been located and (2) that while four of the mirror connections have been made on the basis of comparisons of our observations of the selective population of these ^{19}Ne/^{19}F states in the transfer reactions described in Sec. II C above, five of these connections are made only on the basis of their similar energies and are made only for the purpose of making the rate calculations described below. However, most of these states have a very small single-particle configuration and will be only very weakly populated in resonant proton capture. The most noticeable exception is the level at 6.741 MeV (^{19}Ne); its mirror state at 6.787 MeV ($3/2^-$) in ^{19}F has

TABLE II. ^{18}F+p resonance properties.

Γ_γ (eV) a	Γ_α (eV) a	Γ_{tot} (eV) a	E_x (^{19}F) a	J^π	E_x (^{19}Ne) b	E_r (keV)	Γ_γ (eV) c	Γ_p (eV) d	Γ_α (eV) e	Γ_{tot} (eV)	$\omega\gamma(p,\alpha)$ (eV)	$\omega\gamma(p,\gamma)$ (eV)
[1]	2.8×10^5	2.8×10^5	6.429	1/2-	6.437	26	[1]	6.60×10^{-20}	2.2×10^{5} b	2.2×10^{5} b	2.2×10^{-20}	1.10×10^{-25}
0.85			6.497	3/2+	(?) 6.419	8	0.85	3.50×10^{-34}	$<1\times10^3$	$<1\times10^3$	2.30×10^{-34}	2.00×10^{-37}
0.4		>2.4	6.500	11/2+	?		0.4					
1.2	4.0×10^3	4.0×10^3	6.528	3/2+	(?) 6.449	38	1.2	$2.50\times^{-11}$	4.30×10^3	4.30×10^3	1.70×10^{-11}	5.00×10^{-15}
0.16	1.6×10^3	1.6×10^3	6.554	7/2+	?		0.16					
0.33	7.3	7.6	6.592	9/2+	?		0.33					
5.5	2.4×10^3	2.4×10^3	6.787	3/2-	6.741	330	5.5	6.00 g	2.70×10^3	2.70×10^3	3.5 h	8.10×10^{-3}
0.33	1.2×10^3	1.2×10^3	6.838	5/2+	(?) 6.698	287	0.33	0.27	1.20×10^3	1.20×10^3	2.70×10^{-1}	7.40×10^{-5}
3.1	2.8×10^4	2.8×10^4	6.891	3/2-	?		3.1					
2.4	2.4×10^3	2.4×10^3	6.927	7/2-	6.861	450	2.4	1.60×10^{-2}	3.10×10^3	3.10×10^3	2.10×10^{-2}	1.70×10^{-5}
[1]	5.1×10^4	5.1×10^4	6.989	1/2-	?		[1]					
[1]	8.0×10^{3} f	8.0×10^{3} f	7.100 f	3/2+	(?) 7.070	659	[1]	1.4×10^{4} b	2.5×10^{4} b	3.9×10^{4} b	6.00×10^3	2.40×10^{-1}
[1]	3.2×10^4	3.2×10^4	7.114	7/2+	?		[1]					
0.17	6.7	6.9	7.166	11/2-	(?) 7.173	762	0.17	9.40×10^{-5}	1.20×10^1	1.20×10^1	1.88×10^{-4}	2.66×10^{-6}
[1]	$<6\times10^3$		7.262	3/2+	7.238	827	[1]	$<4\times10^3$	$<6\times10^3$	$<1.0\times10^4$		
[1]			7.364	1/2+	?		[1]					

[a]Reference [4].
[b]Measured (see Table I).
[c]Assuming $\Gamma_\gamma(^{19}$Ne$)=\Gamma_\gamma(^{19}$F$)$.
[d]Assuming $\Theta_p^2=0.1$ for positive parity states and $\Theta_p^2=0.01$ for negative parity states [14].
[e]Assuming $\Theta_\alpha^2(^{19}$Ne$)=\Theta_\alpha^2(^{19}$F$)$.
[f]Reference [10].
[g]$\Theta_p^2=0.03$ [13].
[h]Reference [15].

a spectroscopic factor of $\Theta_p^2=0.03$ [13] and is therefore expected to be reasonably strongly populated in proton capture. The predicted resonance strength for ^{18}F(p,α) is 6 eV which is consistent with the results of a recent direct measurement [15] which yielded a value of $\omega\gamma=2.3\pm1.5$ eV.

Of particular interest is the question of the ^{19}F mirror state corresponding to the 659-keV resonance ($E_x=7.07$ MeV in ^{19}Ne). On the basis of our measured widths and branching ratios, a connection to a $J^\pi=3/2^+$ state at $E_x(^{19}$F$)=7.10$ MeV [10], as suggested by both Rehm *et al.* [8] and Coszach *et al.* [9], would lead to a value of $(\omega\gamma)_{p,\alpha}=6.0$ keV. Rehm *et al.* [8] and Coszach *et al.* [9] independently deduce values of $\omega\gamma=2.7$ keV and 5.6 keV, respectively, based on their direct ^{18}F$(p,\alpha)^{15}$O measurements. Rehm *et al.* [16] have recently set an experimental limit of $\Gamma\gamma\lesssim3$ eV for this level. To try to resolve the questions associated with the existence of this putative $J^\pi=3/2^+$ state (see the end of Sec. II, above), additional studies of the ^{19}F and ^{19}Ne states in this region are currently under way using the ^{12}C$(^{10}$B,^{3}He/$t)$ and ^{15}N(α,γ) reactions.

The stellar reaction rate $N_A\langle\sigma v\rangle$ for a collection of narrow, isolated resonances can be written as (e.g., Ref. [17])

$$N_A\langle\sigma v\rangle=1.54\times10^{11}(AT_9)^{-3/2}\sum_r (\omega\gamma)_r$$

$$\times\exp(-11.605E_r/T_9)\text{ [cm}^3\text{ sec}^{-1}\text{ mol}^{-1}], \tag{3}$$

where A is the reduced mass in amu and where the resonance strength $(\omega\gamma)_r$ and resonance energy (E_r) are in units of MeV. For the ^{18}F$(p,\gamma)^{19}$Ne and ^{18}F$(p,\alpha)^{15}$O reactions,

$$N_A\langle\sigma v\rangle=1.67\times10^{11}(T_9)^{-3/2}\sum_r (\omega\gamma)_r$$

$$\times\exp(-11.605E_r/T_9)\text{ [cm}^3\text{ sec}^{-1}\text{ mol}^{-1}], \tag{4}$$

where the corresponding values of $(\omega\gamma)_r$ and E_r are listed in Table II. Additional terms also have to be included to specifically take into account the contributions of the tails of broad resonances (the 26-keV resonance with $\Gamma\approx220$ keV and the 659-keV resonance with $\Gamma\approx39$ keV), as well as nonresonant direct capture (DC) for the ^{18}F$(p,\gamma)^{19}$Ne reaction. When the slowly varying cross-section factors for these cases are expanded as

$$S(E)=S(0)+S'(0)E+\frac{1}{2}S''(0)E^2, \tag{5}$$

then the resulting reaction rate is given by [17]

$$N_A\langle\sigma v\rangle=N_A(2/\mu c^2)^{1/2}c(kT)^{-3/2}\Delta E_0S_{\text{eff}}(E_0)$$

$$\times\exp(-3E_0/kT), \tag{6}$$

where,

$$S_{\text{eff}}(E_0) = S(0)\left[1 + \frac{5}{12}\frac{kT}{3E_0} + \frac{S'(0)}{S(0)}\left(E_0 + \frac{35}{36}kT\right)\right.$$

$$\left. + \frac{1}{2}\frac{S''(0)}{S(0)}\left(E_0^2 + \frac{89}{36}E_0 kT\right)\right],$$

$$E_0 = [(\mu c^2/2)^{1/2}\pi e^2 Z_1 Z_2 kT/\hbar c]^{2/3} = (0.5184)T_9^{2/3}\ [\text{MeV}],$$

$$\Delta E_0 = 2.309(E_0 kT)^{1/2} = (0.4879)T_9^{5/6}\ [\text{MeV}].$$

For broad resonances, because of the energy dependence of the partial widths, the resonance strength cannot be integrated to give the simple form in Eq. (3). Instead the calculation is carried out including the ''resonance'' contribution (using the widths at E_r) in Eq. (3) and then adding an additional ''tail'' term which includes the effects of the energy dependence of the partial widths (e.g., Ref. [18]). For the $^{18}\text{F}(p,\alpha)^{15}\text{O}$ reaction, the $S(E)$ contributions from the tail of the 659-keV resonances have been calculated in this way and then fit with an expansion as

$$S(E) = 5.5 + 65E + 203E^2\ [\text{MeV b}] \tag{7}$$

(with E in MeV), which can then be integrated to give a reaction rate of the form

$$N_A\langle\sigma v\rangle_{\text{tail}}\ (\text{cm}^3\ \text{sec}^{-1}\ \text{mol}^{-1})$$

$$= 9.13\times 10^{10}T_9^{-2/3}\exp[-18.052T_9^{-1/3} - 0.672T_9^2]$$

$$\times[1 + 0.0231T_9^{1/3} + 6.12T_9^{2/3} + 0.988T_9 + 9.92T_9^{4/3}$$

$$+ 4.07T_9^{5/3}], \tag{8}$$

where the additional $\exp[-0.672T_9^2]$ factor is due to a cutoff term which is used to truncate the tail term in the neighborhood of the resonance [19]. Similarly, for the $^{18}\text{F}(p,\alpha)^{15}\text{O}$ 26-keV resonance,

$$S(E) = 31. - 24.8E - 7.1E^2\ [\text{MeV b}] \tag{9}$$

(with E in MeV), which can then be integrated to give a reaction rate of the form

TABLE III. $^{18}\text{F}+p$ reaction rates.

T_9	$\Sigma(\text{res})$	$N_A\langle\sigma v\rangle$ DC	Total
0.10	3.23×10^{-10}	2.45×10^{-9}	2.77×10^{-9}
0.20	3.24×10^{-5}	4.78×10^{-6}	3.72×10^{-5}
0.30	8.98×10^{-3}	1.83×10^{-4}	9.16×10^{-3}
0.40	1.36×10^{-1}	1.80×10^{-3}	1.38×10^{-1}
0.50	6.59×10^{-1}	9.05×10^{-3}	6.68×10^{-1}
0.60	1.87×10^{0}	3.09×10^{-2}	1.90×10^{0}
0.70	4.04×10^{0}	8.22×10^{-2}	4.12×10^{0}
0.80	7.50×10^{0}	1.84×10^{-1}	7.68×10^{0}
0.90	1.26×10^{1}	3.62×10^{-1}	1.30×10^{1}
1.00	1.98×10^{1}	6.48×10^{-1}	2.04×10^{1}

$$N_A\langle\sigma v\rangle_{\text{tail}}\ (\text{cm}^3\ \text{sec}^{-1}\ \text{mol}^{-1})$$

$$= 5.15\times 10^{11}T_9^{-2/3}\exp[-18.052T_9^{-1/3}]$$

$$\times[1 + 0.0231T_9^{1/3} - 0.415T_9^{2/3} - 0.0670T_9 - 0.0618T_9^{4/3}$$

$$- 0.0254T_9^{5/3}], \tag{10}$$

with no cutoff term needed in this case because the resonance is so far below the Gamov energy E_0. For the $^{18}\text{F}(p,\gamma)^{19}\text{Ne}$ reaction, the effects of such tails turn out to be negligible and were not included.

The nonresonant direct capture to the ^{19}Ne ground state and to its 0.238-MeV and 1.536-MeV excited states was calculated following the formalism of Rolfs [20], adopting a Woods-Saxon potential with a radius parameter $r_0 = 1.26$ fm and a diffuseness of $a = 0.6$ fm. The potential depth was adjusted to reproduce the excitation energies of the final states. Since the single-particle spectroscopic factors for these final states are not known, the $^{18}\text{F}\otimes p$ spectroscopic factors for these states were taken [21] as approximately (within an order of magnitude) equal to the measured $^{18}\text{O}\otimes p$ spectroscopic factors for their mirror states in ^{19}F. The sum of the resulting astrophysical S factors can be parametrized as

$$S(E) = 2.4\times 10^{-3} + 4.1\times 10^{-4}E\ [\text{MeV b}] \tag{11}$$

TABLE IV. $^{18}\text{F}(p,\alpha)$ reaction rates.

T_9	$\Sigma(\text{res})$	$N_A\langle\sigma v\rangle$ 26-keV tail	659-keV tail	Total
0.10	1.10×10^{-6}	2.81×10^{-5}	1.62×10^{-5}	4.54×10^{-5}
0.20	4.13×10^{-2}	5.03×10^{-2}	4.85×10^{-2}	1.40×10^{-1}
0.30	7.94×10^{0}	1.77×10^{0}	2.46×10^{0}	1.22×10^{1}
0.40	1.13×10^{2}	1.61×10^{1}	2.96×10^{1}	1.59×10^{2}
0.50	7.76×10^{2}	7.49×10^{1}	1.72×10^{2}	1.02×10^{3}
0.60	4.31×10^{3}	2.36×10^{2}	6.50×10^{2}	5.20×10^{3}
0.70	1.76×10^{4}	5.75×10^{2}	1.84×10^{3}	2.00×10^{4}
0.80	5.29×10^{4}	1.17×10^{3}	4.27×10^{3}	5.83×10^{4}
0.90	1.25×10^{5}	2.10×10^{3}	8.47×10^{3}	1.36×10^{5}
1.00	2.45×10^{5}	3.38×10^{3}	1.49×10^{4}	2.63×10^{5}

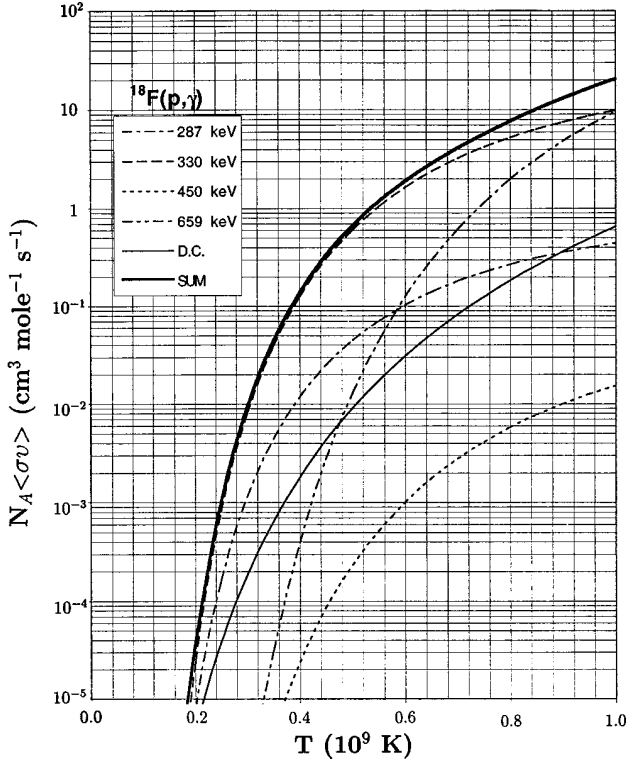FIG. 7. The rate of the $^{18}F(p,\gamma)$ reaction as a function of temperature. Based on the resonance strengths listed in Table II, the contributions of specific resonances are indicated, together with the calculated contribution of nonresonant direct capture. The 330-keV resonance makes the dominant contribution in this temperature range.
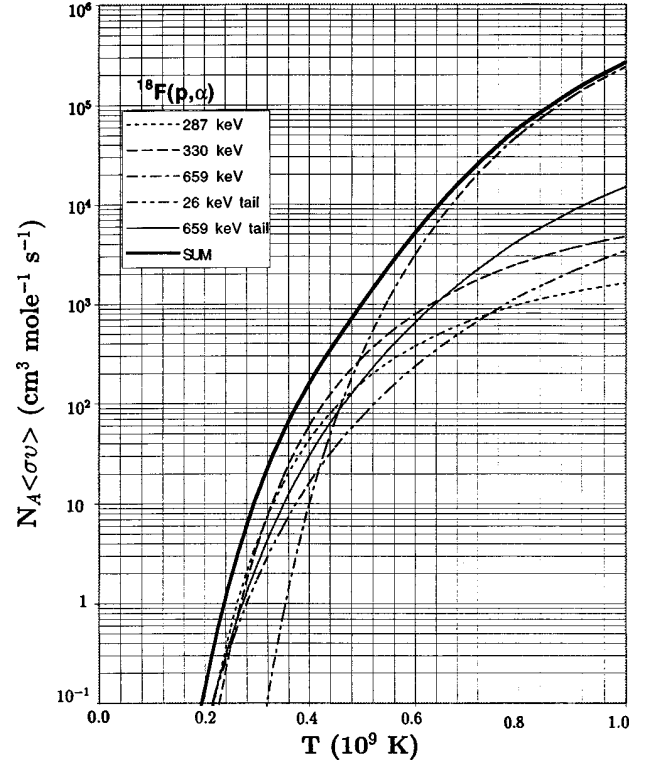

FIG. 8. The rate of the $^{18}F(p,\alpha)$ reaction as a function of temperature. Based on the resonance strengths listed in Table II, the contributions of specific resonances are indicated, together with the contributions due to the tails of the broad resonances at 26 and 659 keV, as described in the text. The 659-keV resonance makes the dominant contribution in this temperature range.

(with E in MeV), which can then be integrated to give a reaction rate of the form

$$N_A \langle \sigma v \rangle_{DC} \ (cm^3 \ sec^{-1} \ mol^{-1})$$
$$= 3.98 \times 10^7 T_9^{-2/3} \exp[-18.052 T_9^{-1/3}]$$
$$\times [1 + 0.0231 T_9^{1/3} + 0.0885 T_9^{2/3} + 0.0143 T_9]. \quad (12)$$

The contributions of each of the various terms (resonances, direct capture, and broad tails) to $N_A \langle \sigma v \rangle$ for the $^{18}F(p,\gamma)^{19}Ne$ and $^{18}F(p,\alpha)^{15}O$ reactions are listed in Tables III and IV as a function of T_9 and are plotted in Figs. 7 and 8. The total reaction rate for each of these reactions is given by the sum of their respective contributions from Eqs. (4), (8), (10), and (12).

IV. ASTROPHYSICAL IMPLICATIONS AND CONCLUSIONS

These results show that in the temperature range $T_9 > 0.5$ [for which the $^{14}O(\alpha,p)^{17}F$ reaction is faster than the $^{15}O(\alpha,\gamma)^{19}Ne$ reaction [22]] the most important (p,α) resonances are the ones at $E_{c.m.} = 330$ and 659 keV, while the most important (p,γ) resonance is the one at $E_{c.m.} = 330$ keV. On the basis of what is currently known about these two resonances, in the range of interest, $T_9 > 0.5$, the $^{18}F(p,\alpha)$ reaction is a few thousand times faster than the $^{18}F(p,\gamma)$ reaction, so that although the $^{14}O(\alpha,p)^{17}F$ reaction is ~ 30 times faster than the $^{15}O(\alpha,\gamma)^{19}Ne$ reaction in this

temperature range, as a breakout from the hot CNO cycle, the $^{15}O(\alpha,\gamma)^{19}Ne$ reaction [23,24] is still ~ 100 times faster than the combination of the $^{14}O(\alpha,\gamma)^{17}F$ [21], $^{17}F(p,\gamma)^{18}Ne$ [25], and $^{18}F(p,\gamma)^{19}Ne$ reactions. However, the following caveats apply to that conclusion: While the properties of the 330-keV (p,γ) resonance are well determined via its isospin mirror in ^{19}F ($E_x = 6.787$ MeV, $J^\pi = 3/2^-$, $\Gamma_\gamma = 5.5$ eV) which has been established in our $^{20}Ne(d,^3He/t)$ measurements, as noted above the properties of the 659-keV resonance are still somewhat ambiguous because its ^{19}F isospin mirror has not been clearly identified. It should also be re-emphasized that there are still at least six missing $^{18}F + p$ resonances in the energy range $0 < E_{c.m.} < 1$ MeV; however, their spectroscopic factors are expected to be small so that they will make only negligible contributions to the reaction rates. To help resolve some of these issues, studies are currently underway (1) using the $^{12}C(^{10}B, t/^3He)$ reaction to search for additional ^{19}Ne states and to try to establish additional $^{19}F \Leftrightarrow ^{19}Ne$ isospin mirror connections and (2) using the $^{15}N(\alpha,\gamma)$ reaction to look for evidence of a $^{19}F(3/2^+)$ state at $E_x \approx 7.1$ MeV.

[1] E.g., G. R. Caughlan and W. A. Fowler, Astrophys. J. **136**, 453 (1962).

[2] R. K. Wallace and S. E. Woosley, Astrophys. J., Suppl. Ser. **45**, 389 (1981).

[3] K. Langanke, M. Wiescher, W. A. Fowler, and J. Görres, Astrophys. J. **301**, 629 (1986).

[4] F. Ajzenberg-Selove, Nucl. Phys. **A475**, 1 (1987).

[5] J. D. Goss, A. A. Rollefson, and C. P. Browne, Nucl. Instrum. Methods **109**, 13 (1973).

[6] R. T. Kouzes, Ph.D. thesis, Princeton University, 1974.

[7] L. M. Martz, S. J. Sanders, P. D. Parker, and C. B. Dover, Phys. Rev. C **20**, 1340 (1979).

[8] K. E. Rehm, M. Paul, A. D. Roberts, D. J. Blumenthal, J. Gehring, D. Henderson, C. L. Jiang, J. Nickles, J. Nolen, R. C. Pardo, J. P. Schiffer, and R. E. Segal, Phys. Rev. C **52**, R460 (1995); K. E. Rehm, M. Paul, A. D. Roberts, C. L. Jiang, D. J. Blumenthal, S. M. Fischer, J. Gehring, D. Henderson, J. Nickles, J. Nolen, R. C. Pardo, J. P. Schiffer, and R. E. Segal, *ibid.* **53**, 1950 (1996).

[9] R. Coszach, M. Cogneau, C. R. Bain, F. Binon, T. Davinson, P. Decrock, Th. Delbar, M. Gaelens, W. Galster, J. Görres, J. S. Graulich, R. Irvine, D. Lebar, P. Leleux, M. Loiselet, C. Michotte, R. Neal, G. Ryckewaert, A. S. Shotter, J. Vanhorenbeeck, J. Vervier, M. Wiescher, and Ph. Woods, Phys. Lett. B **353**, 184 (1995).

[10] H. Smotrich, K. W. Jones, L. C. McDermott, and R. E. Benenson, Phys. Rev. **122**, 232 (1961).

[11] T. Mo and H. R. Weller, Nucl. Phys. **A198**, 153 (1972).

[12] W. R. Dixon and R. S. Storey, Nucl. Phys. **A284**, 97 (1977).

[13] M. Wiescher, H. W. Becker, J. Görres, K.-U. Kettner, H. P. Trautvetter, W. E. Kieser, C. Rolfs, R. E. Azuma, K. P. Jackson, and J. W. Hammer, Nucl. Phys. **A349**, 165 (1980).

[14] M. Wiescher, J. Görres, F.-K. Thielemann, and H. Ritter, Astron. Astrophys. **160**, 56 (1986).

[15] J. S. Graulich *et al.*, Nucl. Phys. **A626**, 751 (1997).

[16] K. E. Rehm *et al.*, Phys. Rev. C **55**, R566 (1997).

[17] W. A. Fowler, G. R. Caughlan, and B. A. Zimmerman, Annu. Rev. Astron. Astrophys. **5**, 525 (1967).

[18] E.g., C. E. Rolfs and W. S. Rodney, *Cauldrons in the Cosmos* (University of Chicago Press, Chicago, 1988), Chap. 4.4.

[19] W. A. Fowler, G. R. Caughlan, and B. A. Zimmerman, Annu. Rev. Astron. Astrophys. **13**, 69 (1975).

[20] C. E. Rolfs, Nucl. Phys. **A217**, 29 (1973).

[21] M. Wiescher and K.-U. Kettner, Astrophys. J. **263**, 891 (1982).

[22] K. I. Hahn, A. García, E. G. Adelberger, P. V. Magnus, A. D. Bacher, N. P. T. Bateman, J. C. Blackmon, G. P. A. Berg, A. E. Champagne, B. Davis, A. J. Howard, J. Liu, B. Lund, Z. G. Mao, D. M. Markoff, P. D. Parker, M. S. Smith, E. J. Stephenson, K.B. Swartz, S. Utku, R. B. Vogelaar, and K. Yildiz, Phys. Rev. C **54**, 1999 (1996).

[23] P. V. Magnus, M. S. Smith, A. J. Howard, P. D. Parker, and A. E. Champagne, Nucl. Phys. **A506**, 332 (1990); P. V. Magnus, M. S. Smith, P. D. Parker, R. E. Azuma, C. Campbell, J. D. King, and J. Vise, *ibid.* **A470**, 206 (1987).

[24] Z. Q. Mao, H. T. Fortune, and A. G. Lacaze, Phys. Rev. C **53**, 1197 (1996).

[25] A. García, E. G. Adelberger, P. V. Magnus, D. M. Markoff, K. B. Swartz, M. S. Smith, K. I. Hahn, N. Bateman, and P. D. Parker, Phys. Rev. C **43**, 2012 (1991).